Stop Treating Diffractions as Noise – Use them for Imaging of Fractures and Karst*

Mark Grasmueck[1], Tijmen Jan Moser[2], and Michael A. Pelissier[3]

[1]Center for Carbonate Research, University of Miami, FL, USA (pmarchesini@rsmas.miami.edu)
[2]Moser Geophysical Services, Den Haag, The Netherlands
[3]Marathon Oil company, Houston, TX, USA

Abstract

Key Findings

- Diffractions are the key to imaging of small-scale discontinuities of carbonate reservoirs and unconventional shale Gas/Oil plays.

- Current reflection seismic survey practice is optimized for continuous stratigraphy but suppresses and collapses diffractions. Quarter-wavelength acquisition and diffraction-friendly processing are needed.

- The combination of high-resolution 3D Ground Penetrating Radar (GPR) outcrop imaging and Ray-Born synthetic modeling helps in deciphering the signatures of unmigrated diffractions.

- Seemingly incomplete and asymmetric diffraction circles visible on timeslices actually contain the dip information of cross-cutting fracture systems.

The reflection seismic method is optimized towards imaging of *continuous* reflectors to delineate stratigraphic boundaries. However, productivity of many carbonate reservoirs and unconventional shale reservoirs is governed by small scale *discontinuities* such as fractures or voids. As a consequence, reflection seismic is of limited use for characterization of discontinuous reservoirs and drilling success rates are

lower than for continuous stratigraphic reservoirs. Fractures and voids are sub-wavelength discontinuities causing diffractions and producing scattered energy on seismic records. Such scatter is commonly regarded as noise and suppressed during acquisition and processing.

Until recently, scattered energy has also prevented clear Ground Penetrating Radar (GPR) imaging of fractured and karstified outcrop analogues. GPR uses electromagnetic waves but has very similar kinematics in terms of reflection, refraction and diffractions. However, by acquiring very dense 3D GPR data with a grid spacing of less than quarter-wavelength in all directions and properly sampling diffractions we have been able to produce images of fractures and karst network with unprecedented resolution and clarity (Pomar, 2010; Grasmueck et al., 2011). Key to producing these images was 3D migration processing to collapse the diffractions. The new work presented here analyzes the *unmigrated* signatures of diffractions. The objective is to better understand the origin of diffractions and investigate their information content in terms of fracture and karst geometry and distribution. Deciphering and verifying the signatures of raw diffractions is supported by Ray-Born synthetic modeling (Moser and Howard, 2008) reproducing the diffraction patterns observed in the 3D GPR field data. The combined findings from modeling and full-resolution 3D GPR data can be used to revise current seismic survey practices for improved imaging of discontinuous reservoirs.

Mostly Assymmetric Diffraction Patterns in 3D GPR Field Data

Capture of the full diffraction signal in seismic and GPR depends on high density data acquisition as shown in Figure 1. The often practiced half-wavelength trace spacing records diffractions as aliased noise. To properly sample the steep dips of diffraction tails denser than quarter-wavelength sampling of the highest signal frequency independent of geological dip is required. The horizontal slice of Figure 2 from the Cassis quarry in France is dominated by diffractions. The perfect circle caused by a point diffractor is a rare exception. The majority of diffractions are asymmetrical. We show in the following sections how this asymmetry of diffractions is a powerful indicator of 3D fracture and karst trends and distribution.

Line Diffraction: Intersection of two Flat Fracture Planes

Diffractions originate from sub-wavelength discontinuities such as edges and corners. When intersecting two thin and flat open fractures the linear intersection causes tipwaves at both ends connected by a linear ridge with a hyperbolic cross section. In the synthetic data timeslice of Figure 3 the tip diffractions show as circles. However, extended linear patterns between diffraction circles cannot be found in the field data (e.g. Figure 2). Natural fractures are not smooth planar features.

Strings of Point Diffractions: A More Realistic Image of Crosscutting Fractures

The linear arrangement of closely spaced diffraction circles with similar radii is the more realistic expression of the vertical fracture intersecting with a horizontal fracture (Figure 3c). On a slightly deeper time slice the circles are transformed into mirrored half circles with a low amplitude corridor in between (Figure 3d). Destructive interference between neighboring point diffractions causes the low amplitude corridor and creates mirrored half circle signatures. Densifying the spacing of the point diffractions along a line would produce the ideal linear diffraction shown in Figure 3b).

If a vertical fracture intersects a dipping subhorizontal fracture the size of adjacent diffraction circles on the timeslice varies (Figure 4). The dip direction of the subhorizontal fracture can be directly determined from the diffraction signature: It points towards the smaller circle.

Fractured and karstified rock generates abundant point diffractions. Natural fractures partition the rock into blocks with sizes above and below the GPR wavelength with many corners (Figure 5). Brittle rock deformation results in conjugate fracture systems. On well-developed fractures small conjugate fractures cause steps and corners acting as wave scatterers. The alignment of such diffractions defines the main fracture trend. Karst dissolution creates voids initiated by fractures. Both karst and fractures are discontinuities and cause similar shapes of diffraction signatures. In the Cassis quarry GPR data karst voids have stronger amplitudes due to their larger opening size compared to fractures and complex shapes with abundant small curvatures.

Vertically Stacked Diffractions are Dip Indicators of Steep Fractures

While Figure 3d illustrates the origin of paired half diffractions, the occurrence of single half circle diffractions (moon shape) is also common (Figure 6). This diffraction signature is caused by vertically stacked diffractions of steeply dipping fractures. The Ray-Born synthetic data show how the diffraction tails are reinforced by parallel superposition above the steep fracture and weakened by wider spacing and destructive interference below. The real data example illustrates the moon shape diffraction signature on a timeslice.

3D Orientation of an Intersecting Fracture System is Encoded in Assymetric Diffraction Cluster

This example unifies the signatures of the individual diffraction signatures discussed above: The model consists of a 60º dipping steep fracture intersected by several subhorizontal fractures dipping 11º with perpendicular dip azimuth to the steep fracture (Figure7). This model corresponds to the main intersecting fracture system of the Cassis quarry. The match of synthetic diffraction signature and the real data signature is very good. The diffraction signature visible on a horizontal slice contains the full geometric information of the quarry fracture network (Figure 8). The alternative approach of interpreting the migrated data by tracking alignments of focused diffraction anomalies took many days to complete. The tell-tale diffraction signatures give away this information on a single timeslice. Asymmetric diffraction circles patterns have also been noticed on timeslices of high-resolution brute stack seismic data near salt domes. The combined synthetic Ray-Born modeling and GPR diffraction signature approach using known fracture and karst configurations of outcrops can be used to decipher the signals from reservoir discontinuities.

Conclusions

Are there less diffractions in seismic than in GPR data? No. The main reason for the apparent lack of diffractions in seismic data is that diffractions are generally suppressed as noise. In order to better harness the seismic information about reservoir discontinuities the following measures should be taken:

- **Acquire dense data** independent of geological dip. Quarter-wavelength sampling

requires i.e. a grid spacing of 5 m for signals of 100 Hz at a near surface velocity of 2000 m/s. Arrivals from deeper seismic events also have to pass the slow shallow surface layer before being sampled.

- **Record single receiver data** instead of hardwired array responses.

- **Acquire more short-offset data** rather than long offset data. Diffractions are omni-directional radiators and excellent velocity indicators.

- **Avoid NMO correction and CMP stacking.** Diffractions are destroyed by these processing steps.

One of the few diffraction friendly processes is 3D migration: Energy is summed along diffraction traveltime curves. Such a new seismic imaging approach is based on adequately recording and processing of the basic point scatterer response. Reflections are automatically included. Following Huygens principle, reflections are the superposition of point scatterer responses. This new seismic/GPR acquisition and processing philosophy makes the best out of diffractions and reflections.

References

Grasmueck, M., M. Coll, G.P.K. Eberli, and K. Pomar, 2011, Diffraction Imaging of Vertical Fractures and Karst with Full-resolution 3D GPR, Cassis Quarry, France: Submitted to Geophysical Prospecting.

Moser, T.J., and C.B. Howard, 2008, Diffraction imaging in depth: Geophysical Prospecting, v. 56, p. 627-641. doi: 10.1111/j.1365-2478.2007.00718.x

Pomar, K., 2010, Visualization and Quantification of Fractures and Karst in Cretaceous Carbonates, Cassis, France: MsC Thesis University of Miami, 105 p.
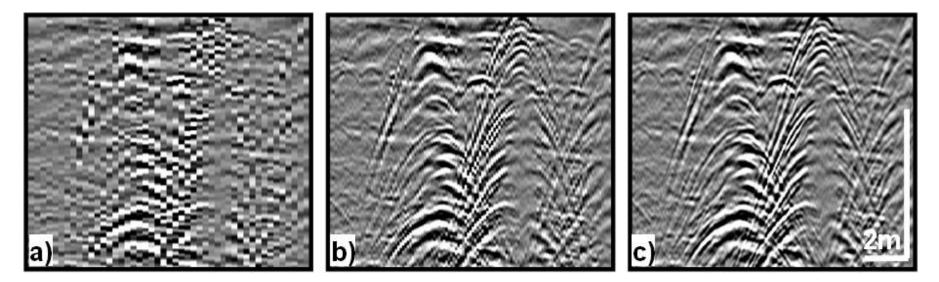
Figure 1. The influence of 200 MHz GPR horizontal trace spacing on spatial sampling of diffractions. (a) At half-wavelength trace spacing of 0.25 m diffraction hyperbolas are spatially aliased and appear as chaotic noise. (b) With quarter-wavelength trace spacing steeply dipping diffraction tails are adequately sampled. (c) At an eighth-wavelength trace spacing of 0.05 m details are further enhanced as also the high frequency spectral content is adequately sampled. Vertical profiles (a) and (b) are generated by decimation of (c).

Figure 2. Unmigrated horizontal slice extracted at 1.95 m depth with abundant diffractions.
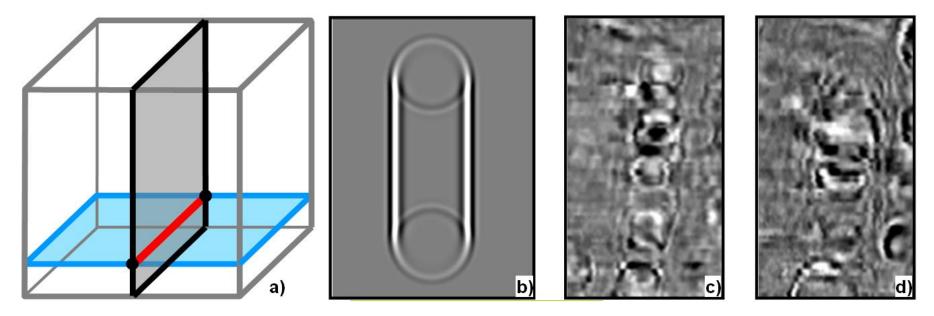
Figure 3. (a, b) Intersection of a vertical and horizontal fracture causes a linear diffraction with two circular tipwaves as seen on a 3D synthetic data timeslice. (c) In real 3D GPR data strings of closely spaced circular diffraction are missing the linear flanks. (d) A deeper time slice of the same diffraction cluster shows mirrored half circles with a lower amplitude corridor in between.
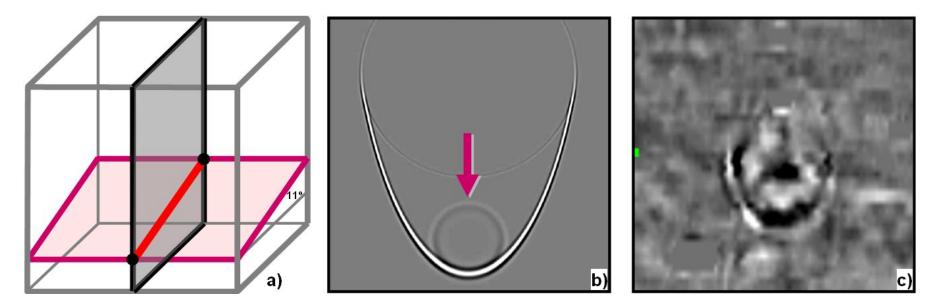
Figure 4. Intersection of a vertical fracture with a 11° dipping subhorizontal fracture causes cascaded diffractions with changing radii on a timeslice extracted from 3D synthetic data. The diffraction signature directly indicates the dip of the subhorizontal fracture. Similar patterns as in (c) are ubiquitous in real 3D GPR data.
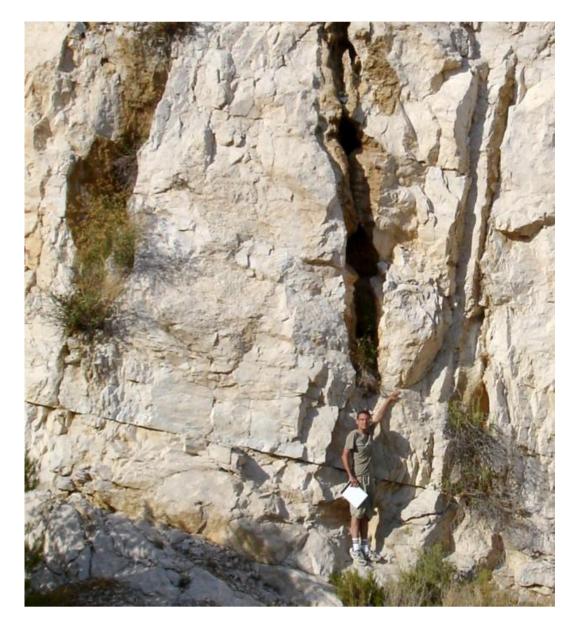
Figure 5. Typical outcrop view of fracture and karst network in the Cassis Quarry. Subvertical fractures are joints with an aperture of less than 1 cm. Fractures are not flat surfaces but are lined with discontinuities creating sharp corners and steps along the main fracture. Subhorizontal fractures dip 11° to the SE and follow bedding planes within the uniform massive limestone. Karst dissolution features are preferentially developed along select subvertical fracture orientations.
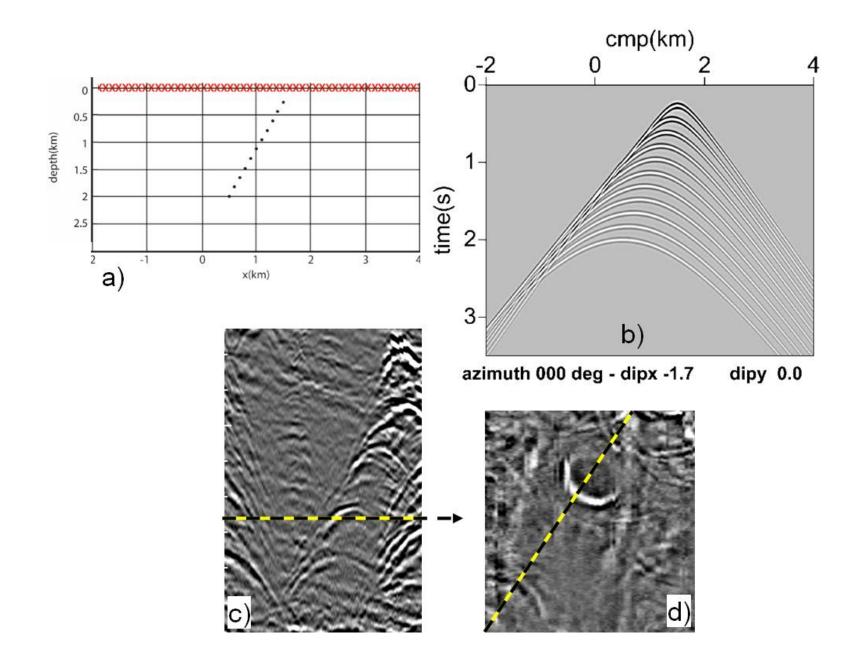
Figure 6. Vertically stacked diffractions caused by steep dip fractures. (a) Model with 11 point diffractors on a 60º slope, and (b) corresponding synthetic data profile. (c) 3D GPR dipline, and (d) timeslice showing moon shaped diffraction signature.
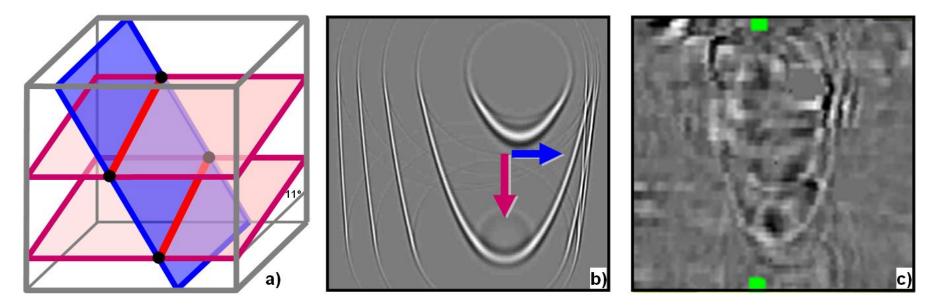
Figure 7. (a, b) Intersection of one vertical and several 11º dipping subhorizontal fractures causes a diffraction signature from which both dip of subvertical and subhorizontal fractures are evident. (c) Real 3D GPR time slice example containing the information about the Cassis quarry main intersecting fractures system.
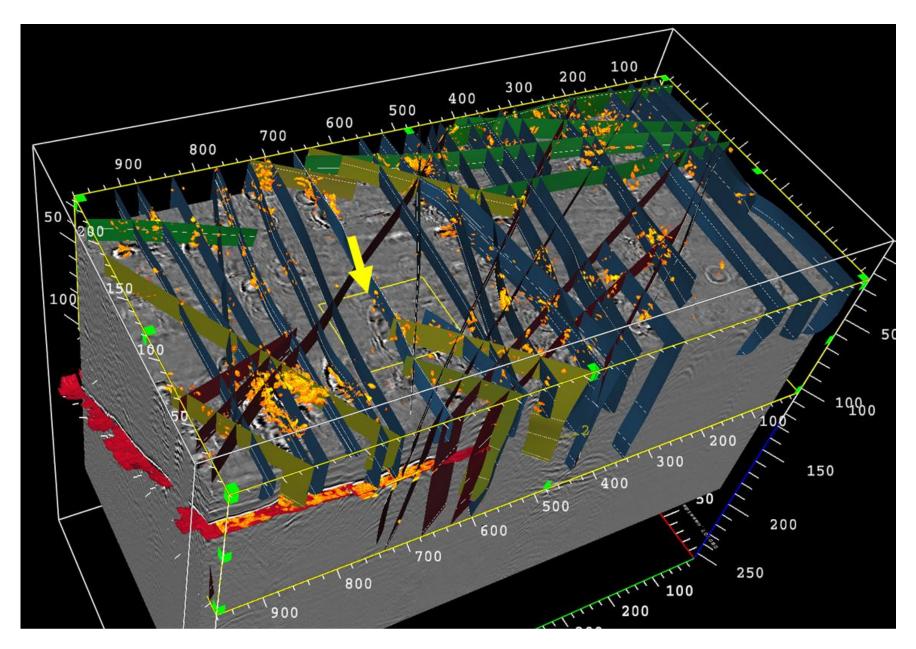
Figure 8. 3D view of the unmigrated Cassis 3D GPR data cube with steep fracture interpretations based on migrated data. Yellow arrow shows the location of diffraction signature shown in Figure 7. Orange colored are volume rendered high amplitude clusters of focused diffractions indicating zones of intense fracturing and karstification.